Journal of Microbiological Methods 162 (2019) 77–82

Contents lists available at ScienceDirect

Journal of Microbiological Methods

journal homepage: www.elsevier.com/locate/jmicmeth

Cyanobacteria as a bioreactor for synthesis of silver nanoparticles-an effect of different reaction conditions on the size of nanoparticles and their dye decolorization ability

Shaheen Husain, Sumbul Afreen, Hemlata, Durdana Yasin, Bushra Afzal, Tasneem Fatma*

Department of Biosciences, Jamia Millia Islamia (Univ), New Delhi 110025, India

ARTICLE INFO

Keywords:
Microchaete sp. *NCCU-342*
Silver nanoparticles
Optimization
TEM
DLS

ABSTRACT

The green synthesis of metallic nanoparticles has paved the way for improving and protecting the environment by decreasing the use of toxic chemicals and eliminating biological risks in biomedical applications. Biological synthesis of metal nanoparticles is gaining more importance due to simplicity, rapid rate of synthesis and eco-friendliness. In the present investigation cyanobacterial (*Microchaete NCCU-342*) cell free aqueous extract has been used for optimizing biosynthesis of silver nanoparticles (AgNP). The optimized reaction parameters for efficient synthesis of AgNP were: biomass quantity of 80 µg/ml, pH 5.5, 60 °C temperature, duration of 60 min UV light exposure and 1 mM $AgNO_3$ concentration. AgNP was characterized by UV–Visible Spectrophotometery, Transmission Electron Microscopy and Dynamic light scattering. The smallest nanoparticles (obtained from biomass parameter were spherical, polydisperessed and in the range of 60-80 nm) were characterized further in a degradation study of azo dye methyl red. Degradation of methyl red within 2 h was more with AgNP (84.60%) as compared to cyanobacterial extract (49.80%).

1. Introduction

Nanotechnology deals with the synthesis of nanomaterials using different systems and their applications. At the nanoscale level, materials have different chemical, physical, optical, magnetic, and electrical properties due to their large surface area to volume ratio (Reddy et al., 2019). At the nanosize sclae penetration potential of particles increases. The plasmonic properties of nanosilver are governed by shape, size, and the surrounding dielectric medium. Metal nanoparticles especially AgNP have been found to be suitable in various applications such as medical diagnosis (Jain et al., 2006), drug delivery systems (Elechiguerra et al., 2005), sanitization (Krishnaraj et al., 2010), water treatment (Prathna et al., 2018) and wound healing (Tian et al., 2007). It has also been used as a bactericidal material in (Hamouda et al., 1999), dental materials (Chladek et al., 2011), a coating material for stainless steel in medical devices (Knetsch and Koole, 2011) and cosmetics (Kokura et al., 2010). Many medical treatments such as intravenous catheters, endotracheal tubes, wound dressings, bone cements, and dental fillings use nanosilver to prevent microbial infections (Sun et al., 2005). Currently, sustainability initiatives that use green chemistry to improve and protect the global environment are becoming focal issues in many fields of research. This has paved the way for the greener synthesis of nanoparticles and has proven to be promising due to slower kinetics, better manipulation, control over crystal growth and their stabilization. This has motivated an upsurge in research on the synthesis routes that allow better control of shape and size for various nanotechnological applications. Instead of using toxic chemicals for the reduction and stabilization of metallic nanoparticles, the use of various biological entities has received considerable attention in the field of nanobiotechnology. Among many possible natural products, biologically active cyanobacterial products represent excellent scaffolds for this purpose (Yasin et al., 2018, 2019; Mubarak Ali et al., 2011; Mahdieh et al., 2012; Roychoudhury and Pal, 2014; Sudha et al., 2013).

Cyanobacterial products play an important role in both reduction and stabilization of nanoparticles. The dyes are a major class of synthetic organic compounds released by many industries such as paper, plastic, leather, food, cosmetic, textile and pharmaceutical industries (Sami and Fatma, 2019; Kulkarni et al., 1985; Zollinger, 1987). These effluents result in significant environmental pollution. Azo dye compounds are recognized as potential carcinogens (Chung and Cerniglia, 1992; Kusic et al., 2011). The dye effluents are highly resistant to microorganisms, thus their reduction by using conventional biological treatment is generally ineffective and also resistant to destruction by physical and chemical treatments at high effluent concentrations. Saha

* Corresponding author.
E-mail address: fatma_cbl@yahoo.com (T. Fatma).

https://doi.org/10.1016/j.mimet.2019.05.011
Received 1 December 2018; Received in revised form 21 May 2019; Accepted 23 May 2019
Available online 24 May 2019

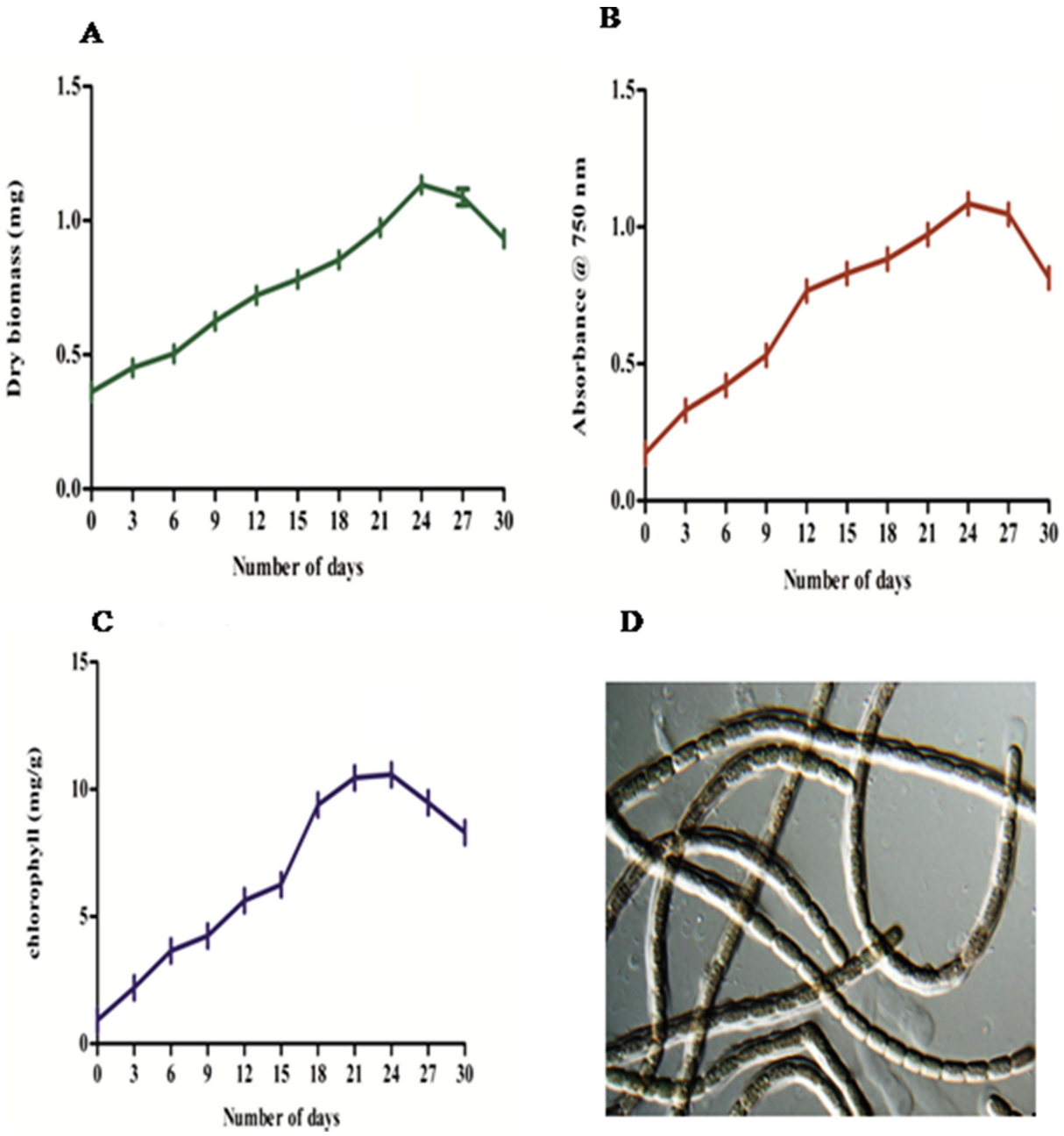

Fig. 1. Growth curve of *Microchaete* adopting different methods A. Gravitational method B. Optical density method C. Chlorophyll estimation method D. Cellular image of *Microchaete*.

et al. (2017) showed methylene blue dye was degraded with AgNP (derived from *Gmelina arborea* tree) within 10 min (Saha et al., 2017). Moreover, Reddy et al. (2016) studied photocatalytic degradation of rhodamine B, methylene blue and phenol by TiO_2/PANI nanocomposite in the presence of UV light.

Due to the emergence of many applications of AgNP in distinct fields, there is an increasing demand of AgNP. To fulfill the demand, there is a pressing need to increase their sources and yield. To achieve this, optimization of their production process is a very important step. So in the present study, we have optimized the AgNP synthesis protocol for size (smallest) and time (quickest) for the degradation of the organic dye, methyl red. To the best of our knowledge, there is no prior report on the *Microchaete* AgNP optimization, characterization and application of dye degradation.

2. Material and methods

Silver nitrate (99.99%) and methyl orange were purchased from Sigma-Aldrich Chemical Co, St. Louis, MO, USA. The remaining analytical grade chemicals were purchased from Merck India. After thorough washing, all glassware was rinsed with distilled water. The *Microchaete* sp. *NCCU-342* was obtained from the Centre for Conservation and Utilization of Blue Green Algae, Indian Agricultural Research Institute, New Delhi and was grown in 500 ml Erlenmeyer flask containing 200 ml BG-11 medium at a light intensity of 2000 ± 200 lux; photoperiod 12:12 h light: dark; temperature 30 ± 1 °C. The cultures were swirled twice a day for aeration and mixing of nutrients. The actively growing starter culture was homogenized and adjusted to an optical density of 0.3 at a wavelength 750 nm and allowed to grow. The growth of the test organism was determined by measuring biomass, chlorophyll and optical density at

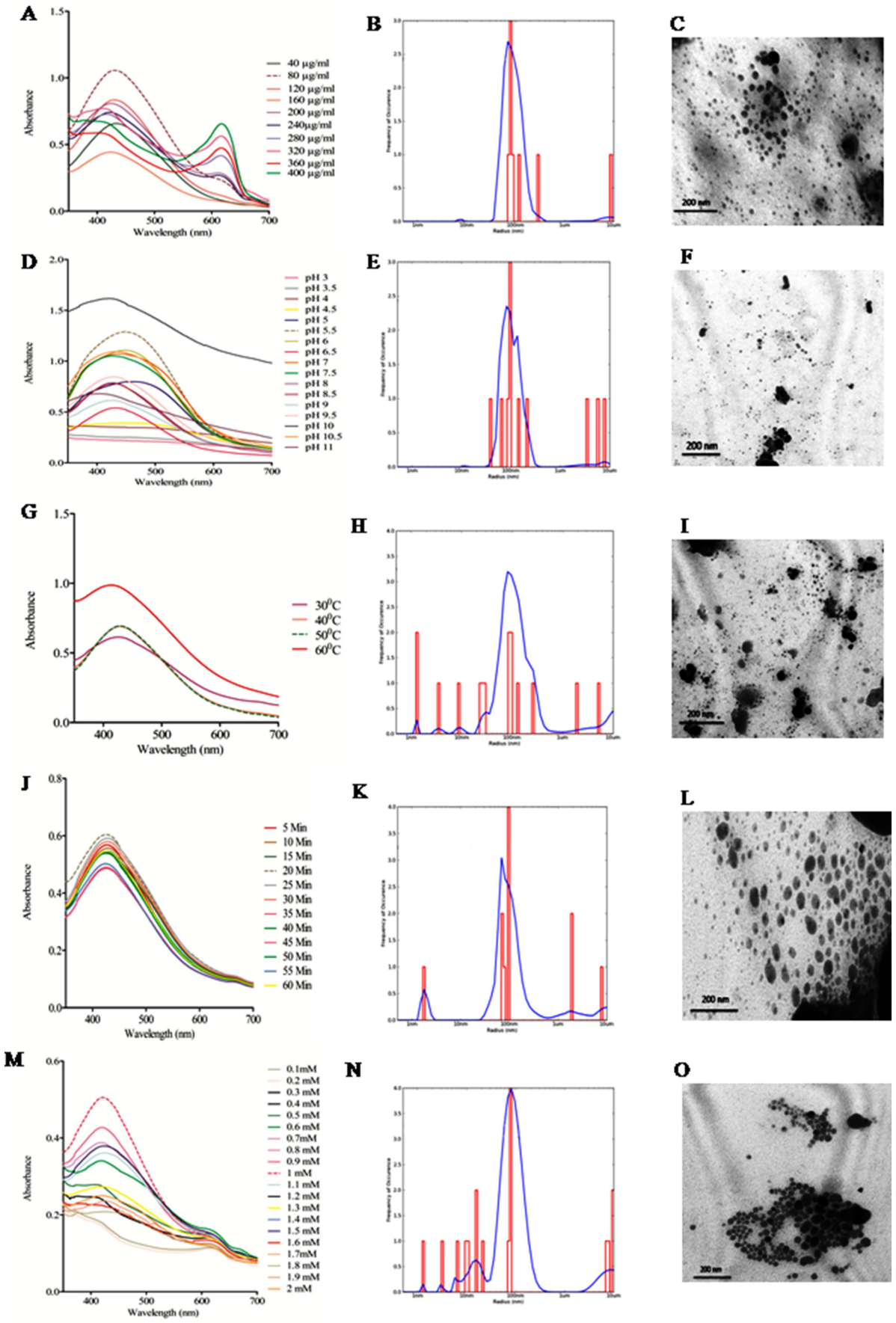

Fig. 2. UV, DLS and TEM images of AgNP synthesized from *Microchaete* A.B.C. Effect of biomass: 80 µg/ml, D.E.F. Effect of pH: 5.5, G.H.I. Effect of temperature: 60 °C, I.J.K. Effect of UV light: 60 min, L.M.N. Effect of Molarity: 1 mM.

750 nm.

After thorough washing with distilled water, biomass was lyophilized and then crushed for powder preparation. This powder (20 mg) was mixed with 10 ml of Milli Q water. The extract was then filtered with Whatman filter paper No. 42. Cell extract (2 ml) was mixed with 1 mM $AgNO_3$ (1 ml) for nanoprticle synthesis. A change in solution color from turbid white to reddish brown indicated AgNP synthesis. To remove any free biomass residue or compound that does not act as the capping ligand of the nanoparticles, the solution with nanoparticles was centrifuged at 10,000 rpm for 10 min at 10 °C using distilled water (five times) (Husain et al., 2015).

For optimization of AgNP biosynthesis *Microchaete* sp. *NCCU-342* cell extract was exposed to various conditions (biomass quantity, pH, temperatures, duration of UV light exposure and $AgNO_3$ concentrations). To check the effect of biomass quantity on synthesis of AgNP, cyanobacterial extract was sampled at different concentrations (1 ml to 10 ml) in 1 ml of $AgNO_3$ (1 mM). Synthesis and stability of AgNP was studied at pH from 3 to 11. The temperature for the best synthesis of AgNP was optimized by incubating the reaction mixture at 30 °C, 40 °C, 50 °C, and 60 °C. Reaction mixtures were also exposed to UV-light for 5 to 60 min at 5 min intervals. In order to optimize the synthesis of the AgNP, the effect of different $AgNO_3$ concentrations (0.1 mM to 2 mM) was also studied.

Physical characterization of synthesized AgNP was done with standard characterization techniques including UV-VIS spectra, TEM and DLS. For UV-VIS spectra, appropriate aliquots were withdrawn from the reaction mixture and the synthesis of AgNP was confirmed. Thin films of the samples were prepared by dropping a very small amount of the sample on the carbon coated grid and then observed by High Resolution Transmission Microscopy (HR-TEM). Dynamic light scattering is an important technique generally used to determine the size distribution pattern of very small particles present in suspension or solution. The DLS technique is widely used for the characterization of particles. The mean diameter of AgNP was determined using the DLS technique with a quartz microcuvette.

To determine the decolorization potential of AgNP a slightly modified protocol of Wong and Yuen (1996) was adopted. The sample was prepared in 50 mmol/ sodium citrate buffer which contained dye solution [Methyl red (50 mg/l)], AgNP (1 mg/ml), Biomass extract (2 mg/ml) and $AgNO_3$ (1 mM Samples were taken at 24 h interval and centrifuged at 8000 rpm for 20 min). The decrease of color intensity was analyzed spectrophotometrically at 430 nm (absorbance maximum for the orange color of methyl red). Methyl red percent dye decolorization was calculated according to the formula:

$$D = 100(Aini - Aobs)/Aini$$

where, D is decolorization (in%), Aini, initial absorbance and Aobs, observed absorbance.

3. Results and discussion

In the present study growth of *Michrochaete* was observed as biomass, chlorophyll and optical density at 750 nm (Fig. 1A, B, C, D). Maximum growth was found on the 24th day in all the methods. Biomass was harvested from the stationary phase cells (24 days old). Shaarika and Nallusam (2015) also found more efficient AgNP synthesis with stationary phase *Bacillus licheniformis*. Due to the large number of emerging applications of AgNP in distinct fields, demand for this method has increased. The first step was to take 10 mg of powder, mix with 10 ml of Milli Q water and keep at 40 °C. After 24 h, extracts were filtered with Whatman filter No. 42. Then 2 ml of extract was added in 1 ml $AgNO_3$ (1 mM) and the prepared sample was kept at 30 °C and pH 6.5 to synthesize AgNP. Synthesis of nanoparticles from cyanobacterial extracts was detected by a change in solution color (pale yellow to blackish brown). After 24 h, appropriate aliquots were withdrawn and the synthesis of AgNP was confirmed by UV–VIS spectroscopy in the range of 300–700 nm (Labtronics LT-2800 spectrophotometer) operated at a resolution of 1 nm as a function of reaction time. Single parameters were optimized at a time, keeping the other parameters constant.

The amount of biomass plays a key role in the reduction of Ag^+ to Ag^o. To optimize the amount of biomass concentrations were varied from 40 μg/ml-400 μg/ml keeping the other parameters constant. In the present study 2 ml extract (80 μg/ml) and 1 ml $AgNO_3$ (1 mM) was found to be best for the AgNP synthesis. The synthesized AgNP showed maximum absorption peak after 24 h at 440 nm (Fig. 2A). No aggregation was seen at this concentration. On increasing concentration of biomass (extract) from 200 to 400 μg/ml the peak shifted toward right (red shift) which indicates the large size of nanoparticles (Morales et al., 2007). TEM micrograph revealed that in 2 ml biomass extract (80 μg/ml) with 1 ml $AgNO_3$ (1 mM) nanoparticles sized ranged between 60 and 80 nm which was also supported by DLS graphs (Fig. 2B, C). Similarly, it was reported that optimal leaf extract, floral petals extract and fungus extract play a significant role in AgNP synthesis. (Dwivedi and Gopal, 2010; Ravichandran et al., 2011; Amit et al., 2012; Krishnaraj et al., 2012; Sonal et al., 2013).

The relationship between the average size of AgNP and the pH values of the solution were investigated. Exposure to the reaction mixture at different pH (3 − 11) showed different responses during AgNP synthesis. The highest and sharpest peak was observed at 450 nm at pH 5.5 (Fig. 2D). It was found that as the pH increases, the peak became broad and shifted toward the right. It is already known, that the optical absorption spectra of metal nanoparticles, shifts to longer wavelength with increasing particle size due to their surface plasmon resonance (Placido et al., 2009). The sensitivity of AgNP synthesis to pH is due to the rate at which the extract releases H^+ ions and donates electrons that reduces silver atoms to their metallic state. When the pH is high, the concentration of H^+ ions in the solution is very low causing fast dissociation of solution particles and simultaneous reduction of a large amount of silver atom, leading to the formation of many nuclei. As a result, the concentration of reduced atoms decreases and the accelerated growth of the nuclei take place to form nanospheres. At neutral pH, the rate at which the solution dissociates is lower and so is the number of nuclei. This allows the available concentration of reduced atoms to be such that some of the nuclei have enough time to grow in to spherical nanoparticles. On the other hand, at low pH the concentration of H^+ ions in the solution is higher causing a slow and progressive dissociation of extract that gives enough time for the formation of large amounts of AgNP (Rodríguez et al., 2017). At pH 5.5, TEM micrograph revealed that the size of AgNP was in the range of 40–100 nm with DLS data also supporting the TEM micrographs (Fig. 2E, F). Moreover the results were in accordance with a previous study in which nanoparticles were synthesized to produce smaller nanoparticles at low pH using cyanobacterial extract (Chakraborty et al., 2009; Dipannita et al., 2012).

Reaction temperature has been considered of great importance (Krishnaraj et al., 2012). Reaction mixtures were maintained at 30 °C, 40 °C, 50 °C and 60 °C. After 24 h, AgNP synthesis increased with increasing temperature and highest peak (440) was observed at 60 °C though it was less sharp than 40 °C and 50 °C (Fig. 2G). The sharpest peak was observed at 50 °C and was selected for further characterization. The result showed that AgNP were spherical and in the range of 40–150 nm (Fig. 2H, I). The enhanced rate of synthesis of AgNP might be the direct result of the effect of temperature on functional groups present in the extract of *Microcheate*. At higher temperature (50 °C and 60 °C) smaller particle size results in sharper plasmon resonance bands of AgNP (Jena et al., 2013; Afreen and Vandana, 2011). The reason for the decrease in particle size with increasing temperature is due to the effect of increased reaction temperature. The reaction rate that consumes silver ions to form nuclei step the secondary reduction process on the surface of the pre-formed nuclei. The size is reduced initially due to the reduced aggregation of the growing nanoparticles. Nam et al.

(2008) also found the same in the peptide mediated synthesis of AgNP. Therefore, by controlling the temperature of the synthetic environment the size of silver nanoparticles can also be controlled.

The optimization of nanoparticles synthesis can be achieved by altering the UV-light exposure as well (Zhen et al., 2013). Reaction mixture was exposed to UV light for 5–60 min at 5 min interval. The peak height increased with increase in UV exposure time. The highest peak was observed after 60 min at 430 nm (Fig. 2J). In principle, radiation with UV light source excited and heated nanoparticles of certain sizes and/or shapes that lead to diffusion and evaporation of surface atoms. Thus, turning the plasmon position accomplishes the characteristics of the nanoparticles. TEM micrographs showed that the size of the nanoparticles were 40–200 nm which was supported by DLS data (Fig. 2K, L). Exposure to UV light significantly altered the size, surface charge, surface chemistry, and dissolution rate of AgNP. Free radical activity (OH·) was identified as a primary mechanism responsible for the surface oxidation of AgNP during UV exposure (Mittelman et al., 2015).

The concentration of $AgNO_3$ plays an important role in the synthesis and size reduction of nanoparticles. Varied concentrations (0.1-2 mM) of $AgNO_3$ in a volume of 1 ml was studied by taking 2 ml biomass extract (80/µg ml), maintained at pH 6.5 and 30 °C temperature. An increase in absorbance of AgNP was observed at concentrations of 1 mM and greater of $AgNO_3$ (Fig. 2M) with a fall in absorbance. The TEM micrographs showed 70–200 nm AgNP with 1 mM $AgNO_3$ and DLS graphs also supported the TEM data (Fig. 2N, O). Previous reports also suggested the maximum absorbance of AgNP with 1 mM $AgNO_3$ (Husain et al., 2015; Jena et al., 2013; Ravichandran et al. (2011). However, Srivastava et al. (2011) and Sonal et al. (2013) reported a maximum yield of AgNP with 0.5 mM and 1.5 mM $AgNO_3$ respectively.

The dye decolorization ability of the AgNP and cell extract of *Microchaete* was assayed regularly against azo dye Methy Red (MR). The decolorization rate of Methy red (50 mg/l) with in 2 h was 84.60% with AgNP (1 µg/ml) and 49.80% from the extract (80 µg/ml) respectively (Fig. 3A, B). There was no decolorization in the control sample (50 mg/l Methy Red and 1 mM $AgNO_3$). AgNP can be successfully used in dye decolorization because of it has a high surface to volume ratio, it is non-toxic and cost effective. It is a novel way to treat several dye pollutants. Further, the literature reveals that the decolorization activity is strongly dependant on the crystal structure, morphology and size of the particles (Jyoti and Singh, 2016; Jyoti and Singh, 2016; Selvam and Sivakumar, 2015). However in our study AgNP (84.60%) showed more decolorization of methyl red as compared to cyanobacterial extract (49.80%) without any mediator within 2 h. These findings showed that MR decolorization reaction became more efficient after the addition of AgNP and the rate of reduction increased with increased concentration of AgNP in the reaction mixture. El-Sheekh et al. (2009) reported that the cyanobacteria *Nostoc lincki* and *Oscillatoria rubescens* removed 82% of methyl red (20 mg/l) after 3 days. Mahmoud et al. (2009) found complete discoloration of methy red from AgNP, AuNP, and AuNP and AgNP co-deposited on SiO_2 NP (50 mg/l) after 70 min, 90 min and 75 min respectively. Other scientists also reported AgNP as a good and highly efficient alternative to decolorize organic compounds and dyes (Kumar et al., 2013; Wang et al., 2007)

4. Conclusion

This study has presented an ecofriendly and inexpensive method for the rapid and large scale synthesis of AgNP using well optimized conditions. To the best of our knowledge there is no report pertaining to the study of the effect of different culture and physical conditions on biological synthesis, of AgNP using cynaobacteria. Culture (effect of biomass) and physical conditions (pH, temperature, UV light intensity and molarity) have been found to affect the maximum yield, rate of synthesis, and size of AgNP. The study also revealed that synthesized AgNP showed appreciable dye decolorization ability as compared to cyanobacterial extract. Thus, AgNP can be used in remediating pollution due to dyes. However, more efforts are needed to employ biological AgNP in environmental remediation.

Acknowledgements

The authors are thankful to University of Chennai, Tamil Nadu for providing the test strains and University Grant Commission India, for providing financial support.

Conflict of interest

Authors declare that there exists no conflict of interest.

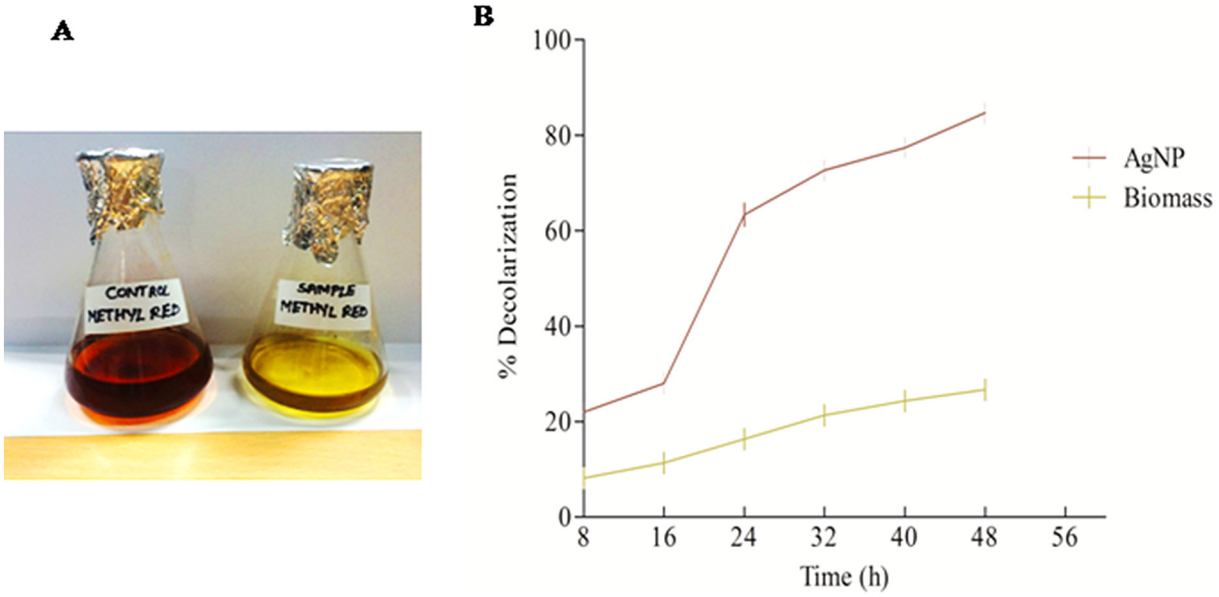

Fig. 3. A.B. Decolorization of organic dye methyl red by AgNP and *Microchaete* after 2 h of incubation. (For interpretation of the references to color in this figure legend, the reader is referred to the web version of this article.)

References

Afreen, B., Vandana, A., 2011. Synthesis and characterization of silver nanoparticles by *Rhizopus stolonier*. Int. J. Biomed. Adv. Res. 2, 148–158.

Amit, K.M., Abhishek, K., Uttam, C.B., 2012. Free radical scavenging and antioxidant activity of silver nanoparticles synthesized from flower extract of *Rhododoendron dauricum*. Nano Biomed. Eng. 4 (3), 118–124.

Chakraborty, N., Banerjee, A., Lahiri, S., Panda, A., Ghosh, A.N., Pal, R., 2009. Biorecovery of gold using cyanobacteria and an eukaryotic alga with special reference to nanogold formation–a novel phenomenon. J. Appl. Phycol. 21, 145.

Chladek, G., Mertas, A., Barszczewska-Rybarek, I., Nalewajek, T., Żmudzki, J., Król, W., Łukaszczyk, J., 2011. Antifungal activity of denture soft lining material modified by silver nanoparticles—a pilot study. Int. J. Mol. Sci. 12, 4735–4744.

Chung, K.T., Cerniglia, C.E., 1992. Mutagenicity of azo dyes: structure-activity relationships. Mut. Res. Rev. Gen. Toxicol. 277, 201–220.

Dipannita, P., Hirak, K., Patra, P., Roychoudhury, A.K., Dasgupta Pal, R., 2012. Gold nanorod production by cyanobacteria—a green chemistry approach. J. Appl. Phycol. 24, 55–60.

Dwivedi, A.D., Gopal, K., 2010. Biosynthesis of silver and gold nanoparticles using *Chenopodium album* leaf extract. Colloids Surf. A Physicochem. Eng. Asp. 369, 27–33.

Elechiguerra, J.L., Burt, J.L., Morones, J.R., Camacho-Bragado, A., Gao, X., Lara, H.H., Yacaman, M.J., 2005. Interaction of silver nanoparticles with HIV-1. J. Nanobiotechnol. 3, 6.

El-Sheekh, M.M., Gharieb, M., Abou-El-Souod, G., 2009. Biodegradation of dyes by some green algae and cyanobacteria. Int. Biodeterior. Biodegradation 63, 699–704.

Hamouda, T., Hayes, M.M., Cao, Z., Tonda, R., Johnson, K., Wright, D.C., Brisker, J., Baker Jr., J.R., 1999. A novel surfactant nanoemulsion with broad-spectrum sporicidal activity against *Bacillus species*. J. Infect. Dis. 180, 1939–1949.

Husain, S., Sardar, M., Fatma, T., 2015. Screening of cyanobacterial extract for synthesis of siler nanoparticles. World J. Microbiol. Biotechnol. 2015. https://doi.org/10.1007/s11274-015-1869-3.

Jain, P.K., Lee, K.S., El-Sayed, I.H., El-Sayed, M.A., 2006. Calculated absorption and scattering properties of gold nanoparticles of different size, shape, and composition: applications in biological imaging and biomedicine. J. Phys. Chem. B 110, 7238–7248.

Jena, J., Pradhan, N., Dash, B.P., Sukla, L.B., Panda, P.K., 2013. Biosynthesis and characterization of silver nanoparticles using microalga *Chlorococcum humicola* and its antibacterial activity. Int. J. Nanomater. Biostruct. 3, 1–8.

Jyoti, K., Singh, A., 2016. Green synthesis of nanostructured silver particles and their catalytic application in dye degradation. J. Genet. Eng. Biotechnol. 14, 311–317.

Knetsch, M.L., Koole, L.H., 2011. New strategies in the development of antimicrobial coatings: the example of increasing usage of silver and silver nanoparticles. Polymers 3, 340–366.

Kokura, S., Handa, O., Takagi, T., Ishikawa, T., Naito, Y., Yoshikawa, T., 2010. Silver nanoparticles as a safe preservative for use in cosmetics. Nanomedicine 6, 570–574.

Krishnaraj, C., Jagan, E., Rajasekar, S., Selvakumar, P., Kalaichelvan, P., Mohan, N., 2010. Synthesis of silver nanoparticles using *Acalypha indica* leaf extracts and its antibacterial activity against water borne pathogens. Colloids Surf. B: Biointerfaces 76, 50–56.

Krishnaraj, C., Ramachandran, R., Mohan, K., Kalaichelvan, P., 2012. Optimization for rapid synthesis of silver nanoparticles and its effect on phytopathogenic fungi. Spectrochim. Acta A Mol. Biomol. Spectrosc. 93, 95–99.

Kulkarni, S.V., Blackwell, C., Blackard, A., Stackhouse, C., Alexander, M., 1985. Textile Dyes and Dyeing Equipment: Classification, Properties and Environmental Aspects. US Government Printing Office.

Kumar, P., Govindaraju, M., Senthamilselvi, S., Premkumar, K., 2013. Photocatalytic degradation of methyl orange dye using silver (Ag) nanoparticles synthesized from Ulva lactuca. Colloids Surf. B: Biointerfaces 103, 658–661.

Kusic, H., Juretic, D., Koprivanac, N., Marin, V., Božić, A.L., 2011. Photooxidation processes for an azo dye in aqueous media: modeling of degradation kinetic and ecological parameters evaluation. J. Hazard. Mater. 185, 1558–1568.

Mahdieh, M., Zolanvari, A., Azimee, A., 2012. Green biosynthesis of silver nanoparticles by *Spirulina platensis*. Sci. Iranica 19, 926–929.

Mahmoud, M.A., Poncheri, A.Y., Badr, A.Y., Abd El Wahed, M.G., 2009. Photocatalytic degradation ofmethyl red dye. S. Afr. J. Sci. 105, 299–303.

Mittelman, A.M., Fortner, J.D., Pennell, K.D., 2015. Effects of ultraviolet light on silver nanoparticle mobility and dissolution. Environ. Sci. Nano 2, 683–691.

Morales, A.E., Mora, E.S., Pal, U., 2007. Use of diffuse reflectance spectroscopy for optical characterization of un-supported nanostructures. Rev. Mexicana Física 53, 18–22.

Mubarak Ali, D., Sasikala, M., Gunasekaran, M., Thajuddin, N., 2011. Biosynthesis and characterization of silver nanoparticles using marine cyanobacterium, *Oscillatoria willei* NTDM01. Digest J. Nanomater. Biostruct. 6, 415–420.

Nam, K.T., Lee, Y.J., Krauland, E.M., Kottmann, S.T., Belcher, A.M., 2008. Peptide-mediated reduction of silver ions on engineered biological scaffolds. ACS Nano 2, 1480–1486.

Placido, T., Comparelli, R., Giannici, F., Cozzoli, P.D., Capitani, G., Striccoli, M., Curri, M.L., 2009. Photochemical synthesis of water-soluble gold nanorods: the role of silver in assisting anisotropic growth. Chem. Mater. 21, 4192–4202.

Prathna, T., Sharma, S.K., Kennedy, M., 2018. Nanoparticles in household level water treatment: an overview. Sep. Purif. Technol. 199, 260–270.

Ravichandran, V., Xin, T.Z., Gunasagaran, S., Xiang, T.F.W., Yang, E.F.C., Jeyakumar, N., Dhanaraj, S.A., 2011. Biosynthesis of silver nanoparticles using mangosteen leaf extract and evaluation of their antimicrobial activities. J. Saudi Chem. Soc. 15, 113–120.

Reddy, K.R., Karthik, K., Prasad, S.B., Soni, S.K., Jeong, H.M., Raghu, A.V., 2016. Enhanced photocatalytic activity of nanostructured titanium dioxide/polyaniline hybrid photocatalysts. Polyhedron 120, 169–174.

Reddy, K.R., Hemavathi, B., Balakrishna, G.R., Raghu, A., Naveen, S., Shankar, M., 2019. Organic conjugated polymer-based functional nanohybrids: synthesis methods, mechanisms and its applications in electrochemical energy storage supercapacitors and solar cells. In: Polymer Composites With Functionalized Nanoparticles. Elsevier, pp. 357–379.

Rodríguez, G.C., Gauthier, G., Ladeira, L., Cala, J.S., Cataño, D.L., 2017. Effect of pH and chloroauric acid concentration on the geometry of gold nanoparticles obtained by photochemical synthesis. J. Phys. Conf. Ser. 935, 012027 (IOP Publishing).

Roychoudhury, P., Pal, R., 2014. Synthesis and characterization of nanosilver—a blue green approach. Indian J. Appl. Res. 4.

Saha, J., Begum, A., Mukherjee, A., Kumar, S., 2017. A novel green synthesis of silver nanoparticles and their catalytic action in reduction of methylene blue dye. Sustain. Environ. Res. 27, 245–250.

Sami, N., Fatma, T., 2019. Studies on estrone biodegradation potential of cyanobacterial species. Biocatal. Agric. Biotechnol. 17, 576–582.

Selvam, G.G., Sivakumar, K., 2015. Phycosynthesis of silver nanoparticles and photocatalytic degradation of methyl orange dye using silver (Ag) nanoparticles synthesized from *Hypnea musciformis* (Wulfen) *JV Lamouroux*. Appl. Nanosci. 5, 617–622.

Shaarika, S., Nallusam, S., 2015. Biosynthesis and characterization of silver nanoparticles produced by *Bacillus lichenifomis*. Int. J. Pharm. Bio Sci. 44, 236–239.

Sonal, S.B., Swapnil, C.G., Aniket, K.G., Mahendra, K.R., 2013. Rapid synthesis of silver nanoparticles from *Fusarium oxysporum* by optimizing physicocultural condition. Sci. World J. 12 Article ID 796018.

Srivastava, A., Kulkarni, A., Harpale, P., Zunjarrao, R., 2011. Plant mediated synthesis of silver nanoparticles using a bryophyte: fissidens minutus and its anti-microbial activity. Int. J. Eng. Sci. Technol. 3.

Sudha, S.S., Rajamanickam, K., Rengaramanujam, J., 2013. Microalgae mediated synthesis of silver nanoparticles and their antibacterial activity against pathogenic bacteria. Indian J. Exp. Biol. 51 (5), 393–402.

Sun, Y., Zhang, Z., Wong, C., 2005. Study on mono-dispersed nano-size silica by surface modification for underfill applications. J. Colloid Interface Sci. 292, 436–444.

Tian, J., Wong, K.K., Ho, C.M., Lok, C.N., Yu, W.Y., Che, C.M., Chiu, J.F., Tam, P.K., 2007. Topical delivery of silver nanoparticles promotes wound healing. ChemMedChem 2, 129–136.

Wang, C.J., Hagemeier, C., Rahman, N., Lowe, E., Noble, M., Coughtrie, M., Sim, E., Westwood, I., 2007. Molecular cloning, characterisation and ligand-bound structure of an azoreductase from *Pseudomonas aeruginosa*. J. Mol. Biol. 373, 1213–1228.

Wong, P.K.Y., Yuen, P.Y., 1996. Decolorization and biodegradation of methyl red by Klebsiella pneumoniae RS-13. Water Res. 30, 1736–1744.

Yasin, D., Fatma, T., Zafaryab, M., Ahmad, N., Aziz, N., Rizvi, M.M.A., 2018. Exploring the bio-efficacies of methanolic extracts of *Nostoc muscorum* and *Calothrix brevissima* with their characterization using GC-MS. Nat. Products J. 8, 305–316.

Yasin, D., Zafaryab, M., Ansari, S., Ahmad, N., Khan, N.F., Zaki, A., Rizvi, M.M.A., Fatma, T., 2019. Evaluation of antioxidant and anti-proliferative efficacy of *Nostoc muscorum NCCU-442*. Biocatal. Agricult. Biotechnol. 17, 284–293.

Zhen, S.J., Zhang, Z.Y., Li, N., Zhang, Z.D., Wang, J., Li, C.M., Zhan, L., Zhuang, H.L., Huang, C.Z., 2013. UV light-induced self-assembly of gold nanocrystals into chains and networks in a solution of silver nitrate. Nanotechnology 24, 055601. https://doi.org/10.1088/0957-4484/24/5/055601.

Zollinger, H., 1987. Synthesis, properties and applications of organic dyes and pigments. Color Chem. 2.